



AFATL-TR-76-122

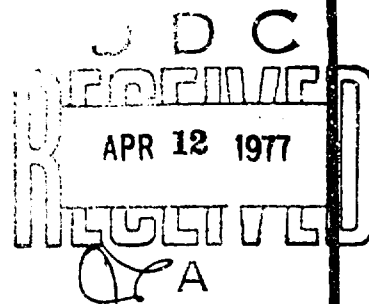
12 2

AD A 038055

STUDIES ON THE PENETRATION MECHANICS OF EGLIN SAND

VULNERABILITY ASSESSMENTS BRANCH
WEAPONS SYSTEMS ANALYSIS DIVISION

OCTOBER 1976



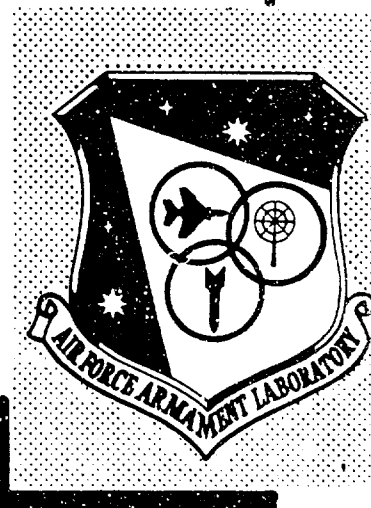
FINAL REPORT-JULY 1976 TO SEPTEMBER 1976

Approved for public release; distribution unlimited

AIR FORCE ARMAMENT LABORATORY

AIR FORCE SYSTEMS COMMAND • UNITED STATES AIR FORCE

EGLIN AIR FORCE BASE, FLORIDA



This Document Contains Page/s
Reproduced From
Best Available Copy

DDC FILE COPY

UNCLASSIFIED

SECURITY CLASSIFICATION OF THIS PAGE (When Data Entered)

REPORT DOCUMENTATION PAGE		READ INSTRUCTIONS BEFORE COMPLETING FORM
1. REPORT NUMBER AFATL-TR-76-122	2. GOVT ACCESSION NO.	3. PERFORMER'S CATALOG NUMBER
4. TITLE (and Subtitle) STUDIES ON THE PENETRATION MECHANICS OF EGLIN SAND.	5. TYPE OF REPORT & PERIOD COVERED Final Report. July 1975 to Sept 1975 1976.	
7. AUTHOR(s) John A. Collins Robert L. Sierakowski	6. PERFORMING ORG. REPORT NUMBER	
9. PERFORMING ORGANIZATION NAME AND ADDRESS Vulnerability Assessments Branch Weapon Systems Analysis Division Air Force Armament Laboratory Eglin Air Force Base, Florida 32542	8. CONTRACT OR GRANT NUMBER(s)	
11. CONTROLLING OFFICE NAME AND ADDRESS Air Force Armament Laboratory Armament Development and Test Center Eglin Air Force Base, Florida 32542	10. PROGRAM ELEMENT, PROJECT, TASK AREA & WORK UNIT NUMBERS Project No. 16 2549 Task No. 11 04 Work Unit No. 004	
14. MONITORING AGENCY NAME & ADDRESS (if different from Controlling Office)	12. REPORT DATE 11 Oct 1976	
	13. NUMBER OF PAGES 29	
	15. SECURITY CLASS. (of this report) UNCLASSIFIED	
16. DISTRIBUTION STATEMENT (of this Report) Approved for public release; distribution unlimited.		
17. DISTRIBUTION STATEMENT (of the abstract entered in Block 20, if different from Report) 62608 F		
18. SUPPLEMENTARY NOTES Available in DDC.		
19. KEY WORDS (Continue on reverse side if necessary and identify by block number) Penetration Mechanics Sand Flash X-rays Poncelet Prediction Sandia Empirical Model		
20. ABSTRACT (Continue on reverse side if necessary and identify by block number) A systematic study of predictive techniques for earth penetration has been reviewed. Based upon this study an industrial proprietary computer code, which appears to be the most flexible and extensible existing model currently available, has been used to examine controlled experimental data generated at AFATL. Results of this data analysis indicate that use of the code requires some judgment in proper selection of input parameters. In addition, test data generated at AFATL indicate that the drag coefficient in predictive soil penetration		

DD FORM 1 JAN 73 1473

EDITION OF 1 NOV 65 IS OBSOLETE

UNCLASSIFIED

SECURITY CLASSIFICATION OF THIS PAGE (When Data Entered)

400936

UNCLASSIFIED

SECURITY CLASSIFICATION OF THIS PAGE(When Data Entered)

(Item 20 continued) equations is velocity dependent over some impact regime and that soil viscosity is an important parameter in this region.

UNCLASSIFIED

SECURITY CLASSIFICATION OF THIS PAGE(When Data Entered)

PREFACE

This report documents work performed during the period from July 1976 to September 1976 by the Vulnerability Assessments Branch, Weapon Systems Analysis Division, Air Force Armament Laboratory, Eglin Air Force Base, Florida 32542, under Project 2549. Messrs. John A. Collins and Robert L. Sierakowski (DLYV) conducted the study for the Armament Laboratory.

This report has been reviewed by the Information Office (OI) and is releasable to the National Technical Information Service (NTIS). At NTIS, it will be available to the general public, including foreign nations.

This report has been reviewed and is approved for publication.

FOR THE COMMANDER

J R Murray
J. R. MURRAY
Chief, Weapon Systems Analysis Division

ADDITION FOR	
NTIS	
000	
UNANNOUNCED	
JUSTIFICATION	
RA	
	CODES
	SPECIAL

A

TABLE OF CONTENTS

Section	Title	Page
I	INTRODUCTION	1
	Purpose and Scope	1
	Background	1
II	EXPERIMENTAL DETAILS	3
	Test Procedure	3
III	THEORETICAL CONSIDERATIONS	9
	Description of Model	9
	Penetration Predictions	11
IV	DISCUSSION	17
V	CONCLUSIONS	20
References		21

LIST OF FIGURES

Figure	Title	Page
1	Blunt-Ended Cylindrical Projectiles	4
2	Experimental Test Set-Up	5
3	Scaled X-Ray of Shot Number 26	6
4	Schematic of Coil Positions	8
5	Coordinate Frames of Reference	10
6	Schematic of X-Ray Positions	12

LIST OF TABLES

Table	Title	Page
1	Experimental Test Matrix	7
2	Comparison of Experimental Data and Predictions - Dry Sand	14
3	Comparison of Experimental Data and Predictions - Wet Sand	15
4	Drag Coefficients Versus Velocity - Wet Sand	19
5	Drag Coefficients Versus Velocity - Dry Sand	19

LIST OF ABBREVIATIONS, ACRONYMS AND SYMBOLS

dF	Elemental Force (kg)
dA	Elemental Area (m ²)
ρ	Medium Density (kg/m ³)
c	Wave Speed of Target Medium (m/sec)
v	Local Absolute Velocity Vector (m/sec)
α	Exponential Decay Factor (1/sec)
t	Time (sec)
τ	Dummy Variable Time (sec)
C _n	Normal Flow Coefficient
C _{τ}	Shear Flow Coefficient
k	A Function of Medium Density and Local Incidence Angle
η	Medium Resistance Coefficient (kg/m ²)

SECTION I

INTRODUCTION

PURPOSE AND SCOPE

The purpose of this study was to use a limited distribution code (specifically, an industrial proprietary code developed by AVCO Corporation) to examine the extent of its predictive capabilities for comparison to experimental data generated at AFATL. In addition, because of the apparent comprehensiveness of the code (three dimensional, six-degrees-of-freedom model) in characterizing penetrator and target, a systematic screening of penetration variables was undertaken to obtain quantitative information on the importance of various properties on penetrator performance.

BACKGROUND

Early studies on determining the penetration mechanics of impacted media have been limited to predictions of the depth of penetrators into target media. In recent years more advanced analytical models have evolved which predict target/penetrator interaction as well as the penetrator trajectory. Although the models introduced appear to have considerable merit, verification of their usefulness has remained somewhat unchallenged due to the limited experimental data available for predictive correlation.

In general, the theories advanced have been categorized in a recent survey (Reference 1) as being of the semianalytical, analytical, theoretical, and empirical type. The semianalytical models include the earliest penetration equations proposed (References 2, 3, 4) and rely to a large extent on experimental data for evaluation of equation constants. The analytical techniques proposed are extensions of the one-dimensional semianalytical models and introduce added target/penetrator constitutive equations for better characterizing penetrator performance. Principal among these models are the cavity expansion theory (Reference 5) and the differential area force law (Reference 6). The cavity expansion theory characterizes the target material compressibility using an elastic-plastic working material model. This analytical technique has been extended (Reference 7) to include such variables as penetrator nose shape, target layering, and impacts deviating at small angles relative to the target surface normal. The range of applicability of such models, however, appears to be limited to essentially normal impact configurations. An apparently more versatile analysis which is based upon a three-dimensional, six-degrees-of freedom model and which includes oblique impact has been introduced in Reference 6. This analytical model considers the penetrator as a rigid body for establishing the loads and accounts for pressure induced drag, target structural resistance, and penetrator surface effects. Once the loads are established by this code, they can be used in

model analysis models or equivalent techniques to estimate loads transmitted to interior penetrator components. Theoretical techniques (References 8, 9, 10) rely upon formulating constitutive equations of the target and penetrator materials for prediction of the governing equation parameters. Many of these techniques, as currently available, are extensions of target penetration codes based upon finite difference or finite element methods, and generally consider symmetric vehicle shapes. While allowing for continuous deformation of both target and penetrator, such computer models involve accurate modelling of the penetrator and target properties for characterizing penetrator performance. Finally, empirical predictions of penetrator performance such as those in Reference 11 have found usefulness for specific velocity regimes and vehicle sizes. Close examination of such predictor equations shows that many of these formulations are modified forms of the one-dimensional classical penetration equations (References 2, 3, 4).

SECTION II

EXPERIMENTAL DETAILS

TEST PROCEDURE

The experimental projectile penetration data recorded has been obtained at the AFATL test range using a facility specifically converted for penetration type testing. The test facility has provisions for adaptation so that both horizontal and vertical firings can be accommodated.

In the present experiments, a series of 0.02 by 0.23 meter long, blunt-ended cylindrical steel projectiles (AISI-W1) (Figure 1) were fired horizontally into a 1.2-meter long by 0.15 meter by 0.40 meter open top box (Figure 2). The test chamber was slowly filled with Eglin sand sieved to remove large debris, using a U.S. Standard Sieve Series Number 25 screen. A 20 millimeter gun was used for firing the projectiles with velocity controlled by the powder charge used. For the present tests, these velocity regimes have been examined for flat-nosed projectiles fired into dry and wet sand targets. The initial impact angle of incidence was approximately zero degrees for all tests. A summary of the specimens tested, with target conditions indicated, is included in Table 1.

In order to obtain data for examining penetrator trajectory through the sand medium, vehicle stability, and forces acting on the projectile, a number of sensing elements were tried and from these several were selected for recording the test data. The most successful of the data collection methods used was found to be flash radiography. For the current experiments five sequentially spaced X-ray heads were used. The first 150 KV unit was located 0.038 meter from the front of the box while the remaining four 300 KV units were spaced 0.38 meter on center from one another. The units were positioned at nominal standoff distances of 0.55 meter from the box center line. To determine the position of the vehicle down the test chamber, a series of letters (A through Q) were attached in a horizontal line along the wall of the box. The letters were spaced at nominal intervals of 0.07 meter with respect to one another and at a distance of 0.20 meter from the top of the box. These letters provided a ready means of locating the horizontal and vertical position of the penetrator in the X-ray record for any instant of time during penetrator motion through the box. In order to detect if any changes in soil motion had occurred during passage of the projectile through the box, a series of 0.0015 meter steel markers were suspended in the soil medium. Both preshot and postshot X-ray records were made to provide this information with Dupont Lightning Plus being used as the X-ray film. An overview of the test chamber, X-rays, and film attached in a test setup is shown in Figure 2, while a scaled schematic of the X-ray's positions in a horizontal plane is shown in Figure 3.

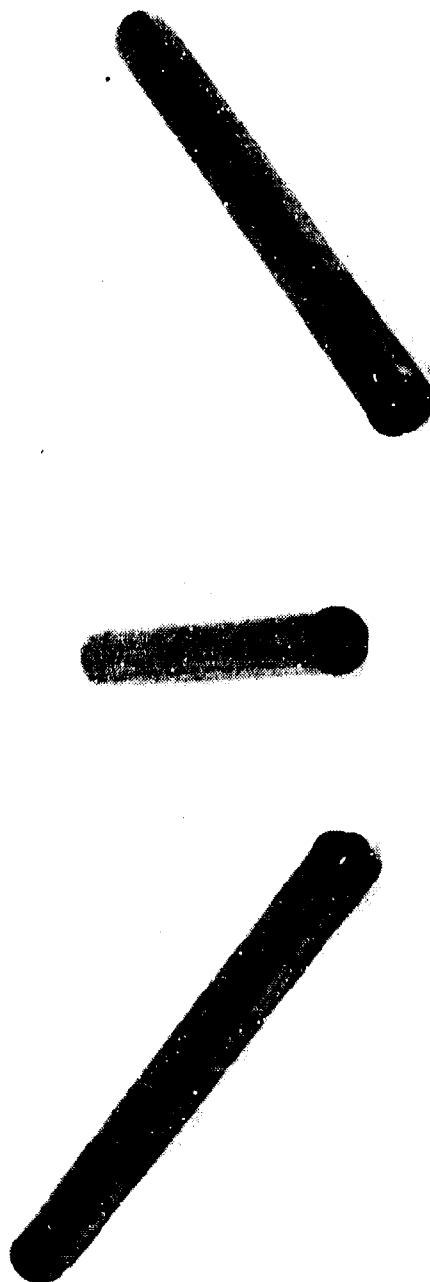


Figure 1. Blunt-Ended Cylindrical Projectiles

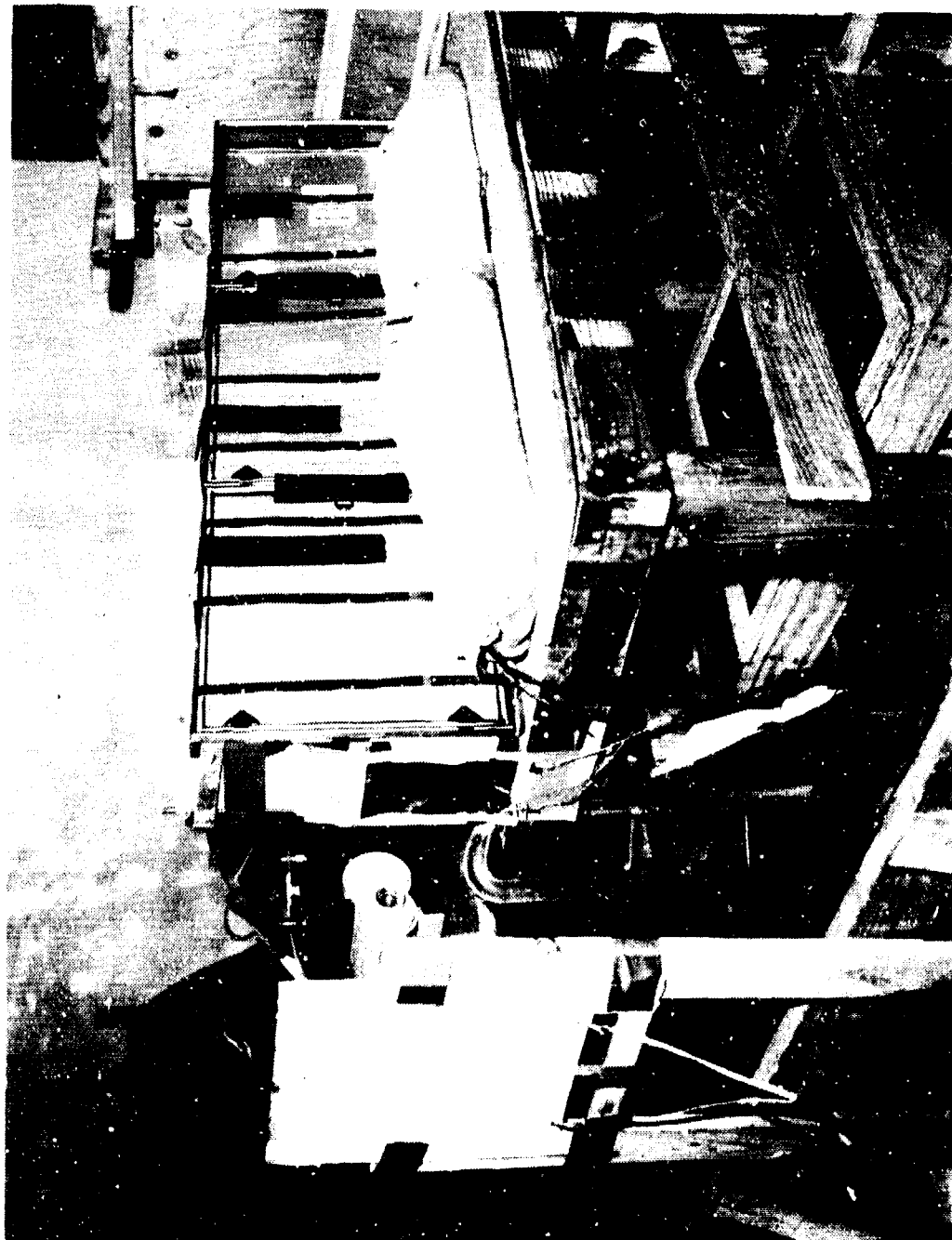


Figure 2. Experimental Test Set-Up



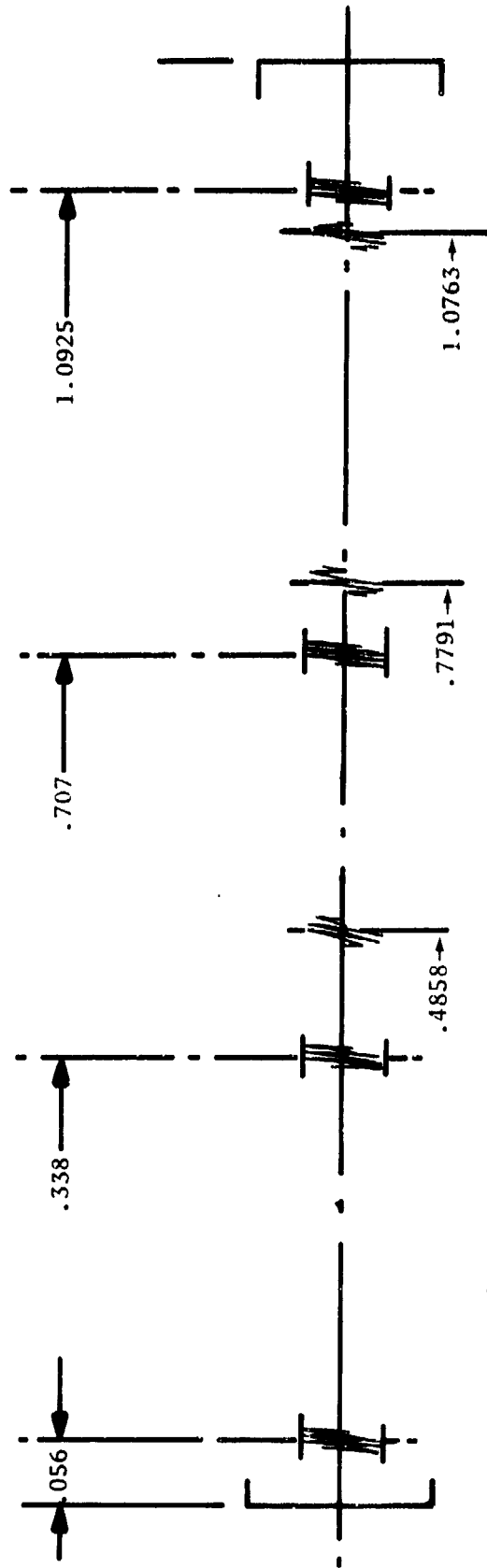
Figure 3. Scaled X-Ray of Shot Number 26

TABLE 1. EXPERIMENTAL TEST MATRIX

Projectile Type	Target	Velocity		
		210 M/Sec	320 M/Sec	400 M/Sec
Flat Nosed	Dry Sand	15 16 17 18 19	20 22 23 24	14 25 26 27 29
Flat Nosed	Wet Sand	70 71 72 73	36 37 38 74 75	76 81 82 83 84

As mentioned, projectile striking velocities were controlled by varying the powder load in a primed 20millimeter case with striking velocity measured, using paper-back velocity screens located at fixed intervals near the test chamber entrance. The X-ray units were triggered by the use of a foil make switch with timing sequence predicted according to best estimates furnished by the Project Engineer.

In addition to the X-ray units, a series of round copper coils were attached to the walls of the test chamber at fixed intervals for use as a further check on projectile velocity while in the test chamber. Such measurements were made possible by magnetizing the projectiles before each test with a nominal field strength of 150 Gauss recorded at the front and tail section of each penetrator. Static measurements were made of projectile motion through the center of the coil to establish peak magnetic response of the projectile while cutting the flux lines. Deviations in peak magnetic response were measured in the order of 0.02 to 0.04 meter in from the nose and tail of the projectile and this range was considered the error bound for the dynamic tests. The size of the coils used (0.15 meter diameter) was determined by trying to insure that the magnetic lines of force would be cut at an optimum position which presumed that the penetrator path was essentially straight and true through the center of the test chamber. For the current vehicle shapes and velocity regimes this was found to be essentially true with errors due to deviations in straight line trajectory and variable location of peak magnetism on the projectile to be of the order of five percent. A schematic of the coil positions used for the tests reported herein is shown in Figure 4.



NOTE: All dimensions in meters

Figure 4. Schematic of Coil Positions

SECTION III

THEORETICAL CONSIDERATIONS

DESCRIPTION OF MODEL

Of the current methods available, the AVCO developed code known in the literature as the differential area force law (DAFL) appears to be the most versatile and represents the only one which can handle non-normal impacts and distributed longitudinal as well as circumferential surface loadings. Although not well documented in the literature, it appears to merit consideration based upon its apparent predictive capabilities.

The form of the DAFL model described here constitutes an extension of previous one- and two-dimensional developments and includes the complete three-dimensional simulation of projectile penetration. The three translational and three rotational equations, which describe the penetrator motion, rely upon knowledge obtained from experiment of certain penetration properties and consider normal as well as non-normal impact simulation. As previously mentioned, such types of models have been classified as semi-analytical. The essential features of this model are outlined in References 6, 12, 13, 14, 15 and 16 and a brief description is included below.

Four coordinate frames of reference are used in the analytical model. These are a fixed inertial frame in the target medium, a target reference frame, a body fixed reference frame at the center of gravity of the projectile, and a pseudo-body reference frame passing through the center of gravity of the projectile. For the initial computations, the projectile is considered as a rigid body moving in a fluid medium (sand) which can be subdivided into a series of surface elements along the circumference of the disk section (Figure 5). The total number of disk sections considered at one time is less than 200, while the number of sector-like segments is greater than six. The sections and sectors together delineate an elemental surface area on which the elemental force acts. This elemental force is considered to be made up of the following components: (1) Normal and shear flow force terms proportional to velocity squared and defined in terms of form and surface drag coefficients, (2) a transient shock term which depends upon the acoustic impedance of the target medium, (3) a cratering term which accounts for the unequal pressure distribution along the length of the projectile, (4) a chipping term which accounts for unequal pressure distribution around the circumference of the penetrator, and (5) a friction term related to the static bearing strength resistance of the target medium. Expressed analytically the DAFL is written as:

$$dF = dA \left[\rho c v e^{-\alpha t} u(t - \tau) + C_n k v^2 + C_t k v^2 + \eta \right] + \text{Target Surface Effects}$$

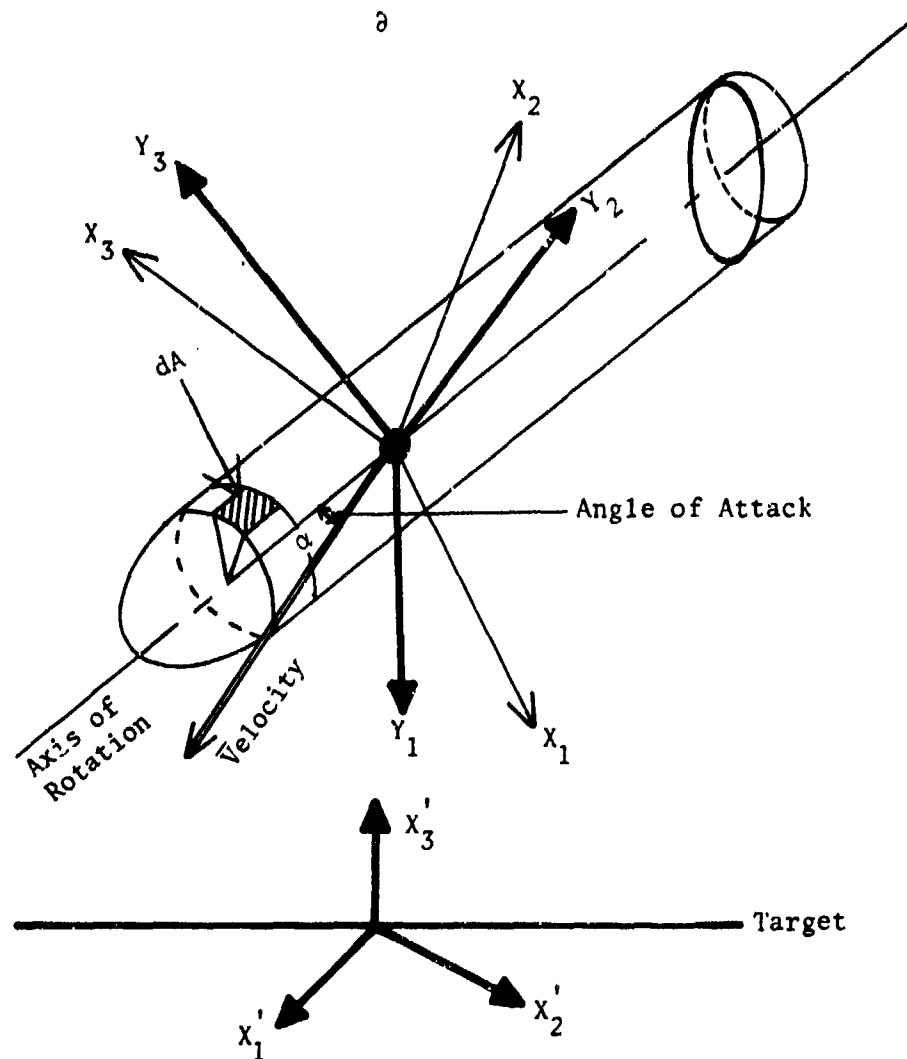


Figure 5. Coordinate Frames of Reference

Each of the elemental force components acting on the respective area elements is transferred to the center of gravity of the vehicle and summed to produce a total resultant force along the body axis. Moments of the differential forces are calculated about the center of gravity of the projectile without the necessity of calculating a center of pressure. Thus, the necessity for introducing other aerodynamic coefficients in addition to the normal and tangential drag coefficients incorporated in the model. Such considerations would appear to enhance the physical completeness of the model and its corresponding predictive capabilities. Specifically, less ambiguity would be introduced into assessing the manner of input associated with the cratering and chipping terms.

The necessity for experimental data as input to the force law becomes readily apparent in the parameters of the terms appearing in the analytical expression. (See List of Abbreviations, Acronyms and Symbols for term identification.) The computer code handles certain standard type nose shapes through attached subroutines; however, other shape types can be handled by substituting specific input information.

PENETRATION PREDICTIONS

As discussed in the experimental section, data on the velocity trajectory of 20millimeter projectiles in dry and wet sand have been obtained at AFATL. With the use of X-ray radiography the trajectory of the impactor can be monitored sequentially with corresponding angle of attack of the projectile recorded. A typical example of the data collected by this technique is shown in Figure 6 which documents Test Number 26 from Table 1. Thus, the data as obtained from these experiments provides an independent basis (other than AVCO's) for testing the DAFL code for predicting the experimental results. In addition, the experimental data obtained coupled with the code predictive capability provides a rational basis for evaluating the significance of individual contributions to the total resultant force.

To initiate data reduction between stations for each shot, the tests indicated in Table 1 were catalogued and data on the striking velocity, projectile position, and time of arrival at the corresponding position recorded. This data was corrected for any photographic distortion in the plane of the projectile by scaling the true vehicle dimensions with respect to the photographically recorded size. This adjusted data was then used to reevaluate and record an adjusted projectile position with subsequent analysis of vehicle velocity, attitude, and other parameters evaluated. Some additional comments related to this data reduction procedure are included in Reference 17. This report also includes a comparison between tests of the one-dimensional form drag flow term in the Poncelet equation versus the corresponding empirical model of Sandia.

The aforementioned data was then used in a Poncelet predictive equation to obtain information on the drag coefficient as a function of velocity which in turn could then be used to determine an arbitrary displacement versus

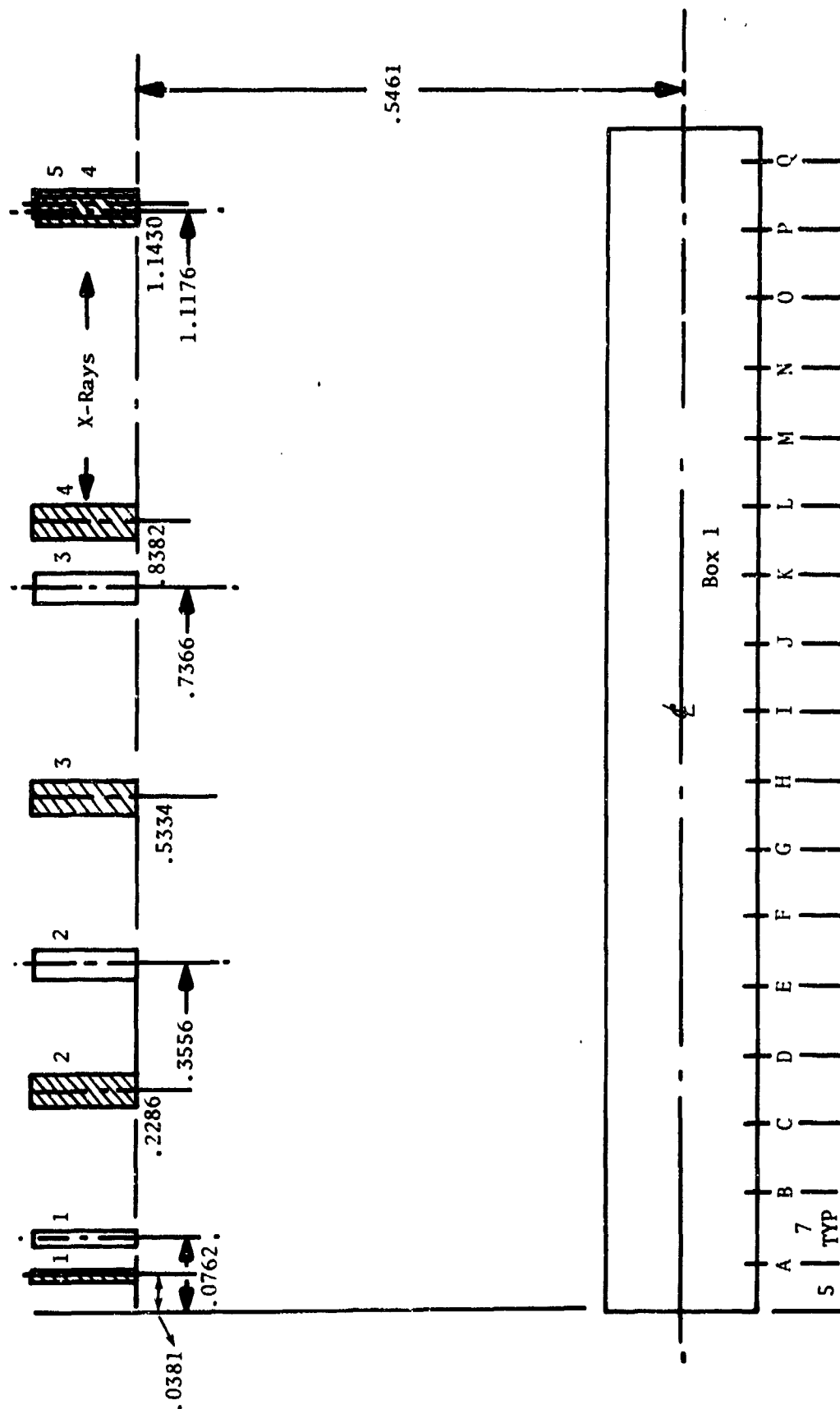


Figure 6. Schematic of X-Ray Positions

velocity and time profile for each shot. A summary of this data is included in Tables 2 and 3 for all of the test cases indicated in Table 1. Since a spectrum of data is indicated in Tables 2 and 3 for each shot, and particulars within each shot, it was possible to establish a drag coefficient versus velocity profile. This information has importance for comparison with available DAFL input information in C_D , C_T versus velocity which is described below.

In order to evaluate the codes predictive capabilities, an examination of one of the AFATL tests described in Table 1 (Number 26) was used as a first reference. To avoid introduction of any input bias, the code was run using the standard table of lookup functions and tabulated data for sand as described in Reference 12. Initial results obtained from the code did not provide satisfactory agreement with the experimental data. Subsequently, an examination of input data for each term was used to systematically screen the influence on and contribution to the total resultant force. As a consequence of the results obtained from the code and for the velocity regime selected for study, it was determined that the flow terms constituted the dominant terms in the force, particularly the drag term. This result had led to a reexamination of the DAFL code input data and to locating an apparent inconsistency in the table of lookup function data for C_N , C_T versus velocity.

On the basis of the AFATL test data a C_D versus velocity lookup function table was constructed and inputted into the DAFL program. In addition, the DAFL code was run using then established table of lookup function data supplied with the code from Picatinny Arsenal for C_D versus velocity with all other input parameters held constant between the two runs. A summary of the results obtained from these runs is included in Tables 2 and 3. As can be seen, the DAFL program run with C_D data extrapolated from the AFATL program provides for very good agreement between code and experimental data. On the other hand, the AVCO tabulated data is shown to provide rather unrealistic predictions on both depth of penetration and resultant velocity.

TABLE 2. COMPARISON OF EXPERIMENTAL DATA AND PREDICTIONS - DRY SAND

Shot No.	Striking Velocity (m/sec)	$\frac{B1}{\left(\frac{\rho A C_D}{2m}\right)}$	Drag (C_D)	Distance (m)	Avg Vel (m/sec)	Cal Vel (m/sec) AVCO	Cal Vel (m/sec) AFATL
16	212.4	0.7621	1.756	0.2723	178.7	at 0.16 = 94.9	171.3
		0.8495	1.958	0.5154	141.3		140.3
17	212.1	0.772	1.779	0.3198	174.1	94.8	164.6
		0.690	1.590	0.5898	139.3		131.7
		0.889	2.049	0.9009	108.6		101.2
18	213.4	0.819	1.887	0.3068	174.6	95.0	167.3
		0.726	1.673	0.5700	139.3		134.7
		1.047	2.413	0.8260	106.5		108.6
19	210.6	0.802	1.849	0.3109	176.5		164.5
		0.816	1.880	0.5728	139.6		132.5
		0.932	1.896	0.8799	106.5		102.2
20	329.2	0.728	1.678	0.2949	268.1	at 0.21 = 96.0	263.2
		0.829	1.910	0.5519	214.8		216.4
		0.732	1.687	0.8621	168.3		169.4
23	328.2	0.874	2.014	0.2990	269.5		261.6
		0.684	1.576	0.5621	216.0		214.1
		0.934	2.152	0.8631	168.7		168.7
24	327.4	0.713	1.643	0.2690	265.9		266.9
		0.770	1.774	0.5250	217.8		219.7
		0.784	1.814	0.8260	172.0		173.4
25	406.0	0.905	2.086	0.2769	329.1		328.3
		0.688	1.400	0.5339	264.2		269.8
		0.794	1.615	0.8321	211.3		214.4
26	406.3	0.774	1.783	0.2799	329.6	at 0.23 = 94.1	328.5
		0.764	1.760	0.5380	266.5		270.1
		0.657	1.515	0.8400	214.0		214.6
27	408.7	0.829	1.909	0.2809	331.4		330.3
		0.749	1.725	0.5380	266.2		271.7
29	405.0	0.839	1.933	0.2809	330.8		327.3
		0.764	1.761	0.5220	266.3		274.0
		0.705	1.625	0.8390	214.0		214.1

TABLE 3. COMPARISON OF EXPERIMENTAL DATA AND PREDICTIONS - WET SAND

Shot No.	Striking Velocity (m/sec)	B1 $\left(\frac{\rho A C_D}{2m}\right)$	Drag (C_D)	Distance (m)	Avg Vel (m/sec)	Cal Vel (m/sec) AVCO	Cal Vel (m/sec) AFATL
70	209.1	1.018	1.7593	0.2741	171.7		171.5
		0.862	1.4897	0.4971	133.6		141.7
		2.0412	3.5276	0.7590	94.4		108.7
71	207.9	1.254	2.1671	0.2680	182.3		171.1
		0.903	1.5605	0.5189	134.2		137.7
		1.112	1.921	0.8260	98.8		99.8
72	214.0	0.7539	1.302	0.2850	181.1		174.9
		0.9035	1.5614	0.5410	142.3		140.7
		0.9681	1.6730	0.8649	104.9		100.5
73	212.8	0.816	1.4102	0.2870	180.9		173.4
		0.745	1.2875	0.5489	143.6		138.5
		0.9818	1.6967	0.8781	108.3		98.0
36	326.2	0.685	1.1838	0.3211	279.0		285.4
		0.517	0.893	0.6060	231.2		248.2
37	336.5	0.656	1.1336	0.2979	279.6		298.1
		0.477	0.824	0.5591	237.0		264.5
		0.705	1.2183	0.8829	196.6		221.7
38	333.1	0.597	1.0317	0.3000	284.0		294.8
		0.535	0.9245	0.5870	240.2		259.6
		0.577	0.997	0.9169	200.1		215.3
74	334.0	0.718	1.2403	0.3091	282.7		294.4
		0.534	0.9228	0.5799	233.4		258.5
		0.712	1.2304	0.9169	189.7		214.6
76	406.0	0.829	1.4326	0.3091	348.2		358.4
		0.379	0.6549	0.5799	291.2		321.3
81	333.8	0.592	1.0229	0.3091	278.7		294.1
		0.5121	0.8850	0.5700	236.6		260.5
		0.757	1.3082	0.8691	193.6		217.2
82	404.8	0.571	0.986	0.3081	343.2		357.5
		0.373	0.6446	0.5621	299.3		322.6
		0.289	0.499	0.8890	269.2		281.2

TABLE 3. COMPARISON OF EXPERIMENTAL DATA AND PREDICTIONS -
WET SAND (CONCLUDED)

Shot No.	Striking Velocity (m/sec)	B1 $\left(\frac{\rho A C_D}{2m}\right)$	Drag (C_D)	Distance (m)	Avg Vel (m/sec)	Cal Vel (m/sec) AVCO	Cal Vel (m/sec) AFATL
83	419.4	0.711	1.228	0.3071	347.0		370.6
		0.3516	0.6972	0.5471	298.5		336.4
		0.664	1.1475	0.8539	258.7		297.0
84	405.7	0.566	0.978	0.3081	333.3		358.3
		0.338	0.5841	0.5441	294.0		325.7
		0.765	1.322	0.8430	253.0		287.8

SECTION IV

DISCUSSION

This study was undertaken to enhance the Air Force in-house capability to realistically predict the terradynamic trajectories of projectile penetration into soil/concrete. Toward this end, development of a test facility from which detailed experimental data could be gathered was assimilated. The principal experimental tool used for obtaining this information was flash radiography. The DAFL three-dimensional code as supplied by Picatinny Arsenal was then run in conjunction with established one-dimensional predictors to simulate the projectile trajectories.

The use and running of the three-dimensional DAFL code at AFATL has resulted in numerous problems. First, the code had been received from Picatinny Arsenal in an interim format, that is, before Picatinny Arsenal believed the code ready for general release. As such, the code was in a nondocumented form without the enhancement of any comment cards and physical explanation. The limited user reports, as available on the DAFL code, also failed to provide adequate information or proper checks for running the code. Nevertheless, with the path trajectory data as reduced from the experimentally obtained X-ray data, the AFATL was in a position to independently examine the DAFL code as well as other predictors.

As can be seen from Tables 2 and 3, the DAFL code predictions did not match the time-position-velocity history data from experiments. It was suggested that this discrepancy might be due to inexperience in running the code which has been indicated to require considerable engineering judgment. This could indeed be the case as there is a lack of documentation and explanation of the code as pointed out, for example, in References 1 and 16. For this reason, a careful study of the DAFL code was initiated. Each component which went into the total force term for each of the modelled penetrator's elemental areas was catalogued. In checking the influence of the various components of the total force for the experimental data available, each term of the total force was systematically compared by suppressing individual component terms. For the case of sand, the shock term, the medium resistance pressure, the shear drag and target surface/edge effects were found to be small in comparison to the fluid dynamic pressure effect denoted in terms of C_N . This latter term was found to be the principal force component responsible for position dependent deceleration in the sand targets tested. This appears to be logical as the projectile was fired into the sand horizontally so that the influence of soil stratification, soil separation and reattachment, and the other principal DAFL terms would not be of concern at these test velocities.

Using the input data for C_N as given in the code, it was found that the DAFL code predicted the projectile velocity to slow down abruptly and then

after it reached approximately one-fifth of its initial value to slowly tend to zero. AVCO has stated that values of C_N can vary from 2.0 at zero velocity to 4.0 at very high velocities (Reference 15). In addition, AVCO states that for purely elastic impact of profile penetrator interaction, where the rebound velocity is equal to the impact velocity, C_N takes on the value 4.0 while $C_T = 0$. A second limiting case is said to occur when $C_N = 2.0$, $C_T = 2.0$ which represents simply purely inelastic momentum transfer. The results of using this data are shown in Tables 2 and 3 under the seventh column. A lack of data in the seventh column indicates that when the code stopped within the computer time limits set forth the vehicle's position (depth) was less than that at which the first X-ray data was obtained.

On the other hand, the AFATL test data also shown in Tables 2 and 3 (second, third and fourth columns) has C_D/C_N varying between 2 at high velocities (inelastic momentum transfer) to approximately 4 at zero velocity (elastic momentum transfer) for dry sand. The inelastic momentum transfer occurs at the higher velocities and is accompanied by the formation of a soil nose when the velocity is high enough. The values of C_D (Tables 4 and 5), as determined by AFATL, have also been found to agree with those reported in References 18 and 19. When these values of C_D (C_N) were used in the DAFL code, that is, varying C_D from 2.0 at high velocities to 4.0 at low velocities in stepwise increments, very good agreement was found between experiment and DAFL code predictions.

Reference 15 includes a discussion on an updated version of the force law coefficients and assigns a new variable C'_D to define an equivalent fluid flow coefficient, specifically,

$$C'_D = C_N \sin^2 \theta + C_T \cos^2 \theta$$

where θ is the average nose cone half angle. In the present AFATL version of the DAFL code, the influence of θ on the corresponding C_N and C_T as a function of velocity must first be calculated before entering this data into the code in the table of lookup functions for $C_N(v)$ and $C_T(v)$. When the velocity vector and the axis of the projectile are non-coincident, the influence of the corresponding nose shape factor may be of some consequence. For the present AFATL experimental data considered in this report, C_N and C_T have been calculated for a specific nose shape, with the corresponding input data related to that case. Specifically, $\theta = 90^\circ$ and therefore C'_D is equal to C_N .

TABLE 4. DRAG COEFFICIENTS VERSUS VELOCITY - WET SAND

V =	0	12.7	25.4	76.2	152.4	228.6	304.8	2540.
C _D	6	4	3	2.2	1.5	1.0	0.7	0.6
AFATL								

TABLE 5. DRAG COEFFICIENTS VERSUS VELOCITY - DRY SAND

V =	0	12.7	25.4	76.2	152.4	228.6	304.8	2540.
C _D	4	3	2.2	2.0	1.9	1.75	1.75	1.7
AFATL								

The shock term analytically represented by $\rho c V u (t - \tau) \exp(-\alpha t)$ was not used in this form in the DAFL code as supplied to the AFATL. The specific form of the shock term used in DAFL is $k v [1 + f_c] u (t - \tau) \exp(-\alpha)$ where the independent variable t has been replaced by the velocity v allowing α to be considered constant with respect to impact velocity. Indeed, as in the preceding case of the nose factor correction, the shock term must be first evaluated to obtain the input data for shock as a function of velocity. When this is done, the input data becomes a special case for V_0 or the striking velocity.

Further, it is observed that the DAFL shock term denoted by FETA 1 is handled within the code as a tabulated lookup function as opposed to a function of the projectile striking velocity. This causes problems in including the influence of a shock term in the DAFL code runs as related to computing the velocity as a function of the depth of penetration. From Tables 2 and 3, it can be seen that the experimentally computed C_D generally starts out high, decreases, and then increases. It would be advantageous to describe the initial penetration by both a drag term and a shock term. The form of this shock term should be of a general form for any target material and should also incorporate functional dependence on velocity and exhibit a characteristic penetration time. Such modifications to the DAFL code as mentioned above will be undertaken in a future study.

Another area which will receive additional study in the future is the low velocity regime. In this regime, the η term or target medium resistance and the medium resistance friction as the soil reattaches to the projectile remain the major influences on vehicle deceleration.

SECTION V

CONCLUSIONS

1. The DAFL three-dimensional, six-degrees-of-freedom code appears to be the best available computer model for predicting projectile penetration in soil.
2. Many items in the DAFL code require a more precise physical description in lieu of the so-called engineering judgment for acceptable understanding and use of the code. Such items as the nose shape factor and shock term are examples that require such considerations.
3. When simulating AFATL test results, with the code, C_D 's varying from 4 to 2 at high velocity for dry sand gave the best results. The inclusion of a shock term for initial impact would most likely have given even better predictive results.
4. For wet sand, C_D varying from six at zero to 0.7 at high velocity gave good simulation. Here again, an initial shock term would have enhanced the predictive results.

REFERENCES

1. G. E. Triandafilidis, State of the Art of Earth Penetration Technology, TR CE-42 (76) DNA-297, May 1976.
2. J. V. Poncelet, Cours de Mecanique Industrielle, First Edition, 1829.
3. M. Petry, Monographics des Systemes d'Artillerie, Brussels, 1910.
4. H. Resal, Sur la Pénétration d'une Projectile dans les Semifluides et les Solides, Paris, 1895.
5. S. V. Hanagud and B. Ross, Large Deformation Deep Penetration Theory for a Compressible Strain Hardening Target Material, AIAA Journal, Vol 9, 1971.
6. D. Henderson and R. L. Stephens, Import and Penetration Technology, Proceedings Fuze-Munitions Environment Characterization Symposium, Picatinny Arsenal, November 1972.
7. R. S. Bernard and S. V. Hanagud, Development of a Projectile Penetration Theory, U.S. Army Engineers Waterways Experiment Station, Penetration Theory for Shallow to Moderate Depth, Technical Report S-75-9, Vicksburg, Mississippi, June 1975.
8. L. D. Bertholf and S. E. Benzley, Toody IIA, A Computer Program for Two-Dimensional Wave Propagation, Sandia Laboratories, SC-RR-68-41, Albuquerque, New Mexico, November 1968.
9. L. J. Hageman and J. M. Walsh, HELP - A Multi-Material Exterior Program for Compressible Fluid and Elastic-Plastic Flows in Two Space Dimensions and Time, Systems, Science and Software, 3S1R-350, Vol 1, La Jolla, California, 1970.
10. R. T. Sedgwick, Theoretical Terminal Ballistic Investigation and Studies of Impact at Low and Very High Velocities, General Electric Company, Space Sciences Laboratory, Technical Report AFATL-TR-68-61, King of Prussia, Pennsylvania, 1968.
11. C. W. Young, Empirical Equations for Predicting Penetration Performance in Layered Earth Materials for Complex Penetrator Configurations, Sandia Laboratories, SC-DR-720523, Albuquerque, New Mexico, December 1972.
12. F. R. Lascher, D. Henderson, T. Stephens, R. Stephens, Projectile Impact and Penetration Forcing Functions Engineering Study, AVSD-0306-73-CR, October, 1972.

REFERENCES (CONCLUDED)

13. F. R. Lascher, D. Henderson, T. Stephens, Determination of Penetration Forcing Function Data for Impact Fuzes - Phase I, AVSD-0074-75-RR, June 1974.
14. R. X. Brennan, Three-Dimensional Impact and Penetration Code Description and Computer Implementation, Picatinny Arsenal, FD and ED IR No. 49, June 1974.
15. F. R. Lascher, D. Henderson, D. Maynard, Determination of Penetration Forcing Function Data for Impact Fuzes - Phase II, AVSD-0306-75-RR, January 1975.
16. P. F. Hadala, Evaluation of Empirical and Analytical Procedures Used for Predicting the Rigid Body Motion of an Earth Penetrator, WES Report No. S-75-15, June 1975.
17. L. E. Malvern, R. L. Sierakowski, J. A. Collins, Studies of the Terradynamics of a Projectile Penetrating Sand Paper to be presented at 47th Shock and Vibration Symposium 19-21, October 1976, Albuquerque, New Mexico.
18. W. A. Allen, E. B. Mayfield, H. L. Morrison, Dynamics of a Projectile Penetrating Sand, Journal of Applied Physics, Volume 28, March 1957.
19. P. R. Hoffman, R. R. McMath, E. Migotsky, Projectile Penetration Studies, AFWL-TR-64-102, December 1964.

INITIAL DISTRIBUTION

HQ USAF/RDQ	1	TAWC/TRADOCLO	1
HQ USAF/SAMI	1	AFIS/INTA	1
Defense Intelligence Agency/DB-4C3	1	Terra Tek	1
AUL (AUL/LSE-70-239)	1	SARP-AD-F-D	2
HQ SAC/NRI	1	DRXBR-TE	2
Nav Wpns Center/Code 3269	1	AMXBR-VL	1
Nav Wpns Center/Code 603	1	BRL/Tech Library	1
Nav Wpns Center/Code 533	1	AVCO Corporation	2
Nav Wpns Center/Code 407	1		
AFSC Liaison Office/Code 143	2		
Ogden ALC/MMWM	2		
AFATL/DLOSL	9		
AFATL/DL	1		
AFATL/DLJK	1		
AFATL/DLJW	1		
AFATL/DLD	1		
AFATL/DLY	1		
ADTC/XR	1		
ADTC/SD	2		
SACPO	1		
USAFTAWC/OA	1		
AFATL/DLYV	10		
AFATL/DLYW	1		
Southwest Research Institute	1		
Orlando Technology Inc.	1		
Sundstrand Data Contro, Inc.	1		
Texas Tech University	2		
Univ of Florida Grad Center	3		
Univ of Florida/Engrg Sciences	7		
US Army Engrg Waterways Experiment Station	2		
Defense Nuclear Agency/SPSS	3		
Goodyear Aerospace Corp/Dept 456	1		
Sandia Laboratories	2		
Lawrence Livermore Laboratory	1		
Martin Marietta Aerospace	1		
Georgia Institute of Technology/ Dept of Aerospace Engrg	1		
University of New Mexico	2		
US Army Material Systems Analysis Agency/R&D Center	1		
DDC	12		
Oklahoma State University	1		
Lockheed Missiles & Space Co., Inc/ R&D Division	1		
ASD/ENFEA	1		

This Document Contains Page/s
Reproduced From
Best Available Copy